JOURNAL OF PHYSICAL ORGANIC CHEMISTRY
J. Phys. Org. Chem. 2003; **16:** 772–782
Published online in Wiley InterScience (www.interscience.wiley.com). DOI: 10.1003/poc.644

Novel cadmium–organic frameworks with nitrilotriacetate†

Filipe A. Almeida Paz and Jacek Klinowski*

Department of Chemistry, University of Cambridge, Lensfield Road, Cambridge CB2 1EW, UK

Received 31 January 2003; revised 12 March 2003; accepted 13 March 2003

epoc ABSTRACT: Novel cadmium–organic frameworks incorporating nitrilotriacetate (NTA^{3-}) and BPY (4,4′-bipyridine) were synthesized under hydrothermal conditions and structurally characterized by single-crystal x-ray crystallography and other techniques. The crystal structure of CUmof-7, $[Cd_4(BPY)_5(NTA)_2(H_2O)_4]\cdot(NO_3)_2\cdot(H_2O)_x$, , consists of infinite 2D cationic bilayers stacked along the *c* direction, and perforated by wide tubular channels filled with nitrate ions and highly disordered water molecules. CUmof-8, $[Cd_4(BPY)_4(NTA)_2(H_2O)_{10}]\cdot(BPY)\cdot(NO_3)_2\cdot(H_2O)_8$, is a 1D metal–organic polymer produced by the self-assembly of a bimetallic secondary building unit into a cationic chain, $[Cd_2(BPY)_2(NTA)(H_2O)_5]_n^{n+}$. NTA^{3-} appears in both crystal structures as an effective polydentate ligand which traps the Cd^{2+} metal ions inside three chelate five-membered rings, eliminating available coordination sites and favouring the formation of 1D polymers (for CUmof-8). Copyright © 2003 John Wiley & Sons, Ltd.
Additional material for this paper is available from the epoc website at http://www.wiley.com/epoc

KEYWORDS: O-ligands; supramolecular chemistry; crystal engineering; cadmium; coordination polymers

INTRODUCTION

Crystal engineering of metal–organic frameworks (MOFs), a growing area of research in the field of supramolecular chemistry, leads to novel scaffolding architectures and topologies.[1,2] The use of metal centres with specific coordination geometries and selected organic ligands allows the syntheses of highly ordered structures, which can incorporate properties of both purely organic and inorganic compounds. Much work has been devoted to the use of multitopic ligands capable of forming bridges between two or more metal centres. Rod-like *N*,*N*′-donor ligands, such as 4,4′-bipyridine (BPY), and molecules containing two or more *exo*-carboxylic acid groups able to coordinate to several metal centres in various modes, have been successfully employed in the synthesis of multidimensional MOFs.[3–6] A great variety of novel materials showing interesting properties and potential applications for reversible guest exchange,[7–9] catalysis,[10,11] photoluminescence,[12–15] unusual magnetic and non-linear properties,[16–20] chirality[21–23] and clathration[24,25] have been reported.

Because of the complexity of the crystal structures, the structural characterization of MOFs heavily relies on single-crystal analysis and is therefore very sensitive to the quality of the crystalline product. The mechanism of crystallization in solution can be described as a series of successive molecular recognition events between metal and ligands, leading to the spontaneous self-assembly in one-, two- or three-dimensional space. In aqueous media, the substitution of water in the coordination sphere of aquo complexes by donor atoms from multitopic organic ligands is normally highly favourable thermodynamically (increased entropy). The high strength of the resulting coordinative bonds and fast kinetics for nucleation and crystal growth are the main causes of irreversible nature of the crystallization events, leading to the formation of poorly crystalline compounds.[26,27] Hydrothermal synthesis routes of novel MOFs at high temperature and pressure are difficult and poorly explored. However, they can lead to highly crystalline products via careful control of the temperature profile used for the synthesis,[28] and improved solubility of heavy organic molecules in water. This can overcome the high activation energies necessary to start nucleation, leading to the formation of very rare and interesting complex metastable phases. On the other hand, the same metastable compounds are usually thermodynamically very unstable and thus difficult to isolate.

We have focused on the synthesis of novel highly crystalline MOFs which incorporate the so-called traditional ligands together with molecules novel to the field.[28–31] Recently, we reported the first MOF incorporating a multidentate chelating organic ligand, $[Cd_4(HDTPA)_2(BPY)_3(H_2O)_4]\cdot 14H_2O$ (CUmof-2, where

**Correspondence to:* J. Klinowski, Department of Chemistry, University of Cambridge, Lensfield Road, Cambridge CB2 1EW, UK.
E-mail: jk18@cam.ac.uk
†Dedicated to Professor Dr Tadeusz Marek Krygowski on the occasion of his 65th birthday.
Contract/grant sponsor: Fundação Para a Ciência e Tecnologia.
Contract/grant number: SFRH/BD/3024/2000.

$HDTPA^{4-}$ is *N*″-carboxymethyldiethylenetriamine-*N*,*N*,*N*′,*N*″-tetraacetate), which can direct the dimensionality of the final crystal structure.[29] Just like $HDTPA^{4-}$, nitrilotriacetic acid (H_3NTA) is also a precursor of a multidentate organic ligand (NTA^{3-}), incorporating carboxylic acid groups and one *N*-donor atom, capable of coordinating to several metal centers and also of eliminating available coordination sites. Surprisingly, a search in the Cambridge Structural Database[32] produced only a few one-,[33–38] two-[38,39] and three-dimensional[40–42] MOFs with H_xNTA residues. We felt that this molecule could be used as a building block in the construction of novel crystal structures with characteristics similar to CUmof-2. We report here the synthesis, crystal structure and determination of the first one-dimensional (1D) and two-dimensional (2D) cadmium–organic frameworks (Cd–OFs) incorporating NTA^{3-} and BPY: CUmof-7 has a 2D $[Cd_4(BPY)_5(NTA)_2(H_2O)_4]_n^{2n+}$ cationic bilayer perforated by large tunnels which run in one direction and contain highly disordered water molecules; CUmof-8 is a 1D cationic polymer, $[Cd_2(BPY)_2(NTA)(H_2O)_5]_n^{n+}$, with striking topological similarities to CUmof-2.[29]

SYNTHESES

All reagents were readily available from commercial sources and were used as received.

Synthesis of $[Cd_4(BPY)_5(NTA)_2(H_2O)_4]\cdot(NO_3)_2\cdot(H_2O)_x$ and $[Cd_4(BPY)_4(NTA)_2(H_2O)_{10}]\cdot(BPY)\cdot(NO_3)_2\cdot(H_2O)_8$

To a solution of $Cd(NO_3)_2\cdot 4H_2O$ (0.333 g, Aldrich) in distilled water (ca 6.5 g), 4,4′-bipyridyl (BPY, 0.160 g, Aldrich), nitrilotriacetic acid (H_3NTA, 0.240 g, Aldrich) and triethylamine (TEA, 0.280 g, Avocado) were added and the mixture was stirred thoroughly for 1 h at ambient temperature. The suspension, with a molar composition of 1.05 : 350 : 1.00 : 1.23 : 2.70, respectively, was transferred to a Parr PTFE-lined stainless-steel vessel (8 cm^3, filling rate 70%) and placed for 3 h at 145 °C in a preheated oven. The reaction vessel was allowed to cool slowly to ambient temperature at a rate of 10 °C h^{-1}, giving a white microcrystalline product from which very small crystals of $[Cd_4(BPY)_5(NTA)_2(H_2O)_4]\cdot(NO_3)_2\cdot(H_2O)_x$ (CUmof-7) were separated. The suspension was placed in a refrigerator at 4 °C and the solvent allowed to evaporate slowly over a period of 16 weeks, after which CUmof-7 was converted into small crystals identified as $[Cd_4(BPY)_4(NTA)_2(H_2O)_{10}]\cdot(BPY)\cdot(NO_3)_2\cdot(H_2O)_8$ (CUmof-8). These were manually separated and air-dried at 70 °C. This Cd–OF proved to be air- and light-stable, and insoluble in water and common organic solvents such as methanol, ethanol, acetone, dichloromethane, toluene and chloroform.

Structural characterization of CUmof-8

Elemental composition found: C 36.35, H 3.75, N 9.38%. Calculated (based on single-crystal data): C 36.24, H 4.32, N 9.54%.

TGA data (weight losses): 20–115 °C 15.7% (DTG peak at 71 °C); 115–225 °C 13.7% (DTG peaks at 164 and 188 °C); 225–296 °C 14.2% (DTG peak at 240 °C); 225–334 °C 18.7% (DTG peak at 316 °C); 334–500 °C 12.8% (DTG peak at 370 °C).

Selected FT-IR data (cm^{-1}): ν(O–H, water) = 3393 vs (and very broad); ν(C–H, aromatic compounds) = 3054 m; ν(C–H in —CH_2—) = 2903 m; overtones and combination bands for 4-monosubstituted pyridines = 1942 w, 1767 w and 1650 s; $\nu_{asym}(CO_2)$ = 1602 vs and 1574 vs (and broad); ν(=C–H, aromatic compounds) = 1533 m and 1489 w; $\nu(NO_3^-)$ = 1436 m (very broad); $\nu_{sym}(CO_2)$ = 1412 vs and 1385 vs; δ(O–H···O) = 1357 s (broad) and 1327 m; ν(C–O) = 1257 m (broad); δ(=C–H, 4-monosubstituted pyridines) = 1219 m and 1074 m; ρ(=C–H) = 1129 m and 1043 m; ring breathing modes (C=C plus C=N) = 1025 w and 1006 m; 994 m; γ(O–H···O) = 926 m and 905 m; γ=(C–H, 4-monosubstituted pyridines) = 855 w, 834 ws, 807 vs; γ(C=O) 726 m; δ(C=C, pyridyl groups) = 629 s; δ(C–N–C, tertiary amines) = 533 m; ρ[(C=O)–O] = 490 m.

Selected FT-Raman data (cm^{-1}): ν(=C–H, aromatic compounds) = 3079 m; $\nu_{antisym}$(=C–H) and ν_{sym}(=C–H) = in the 2932 w region; ν(C=O) and ν(C=C plus C=N from 4-monosubstituted pyridines) = 1616 s and 1603 m; ν(=C–H, aromatic compounds) = 1518 m; typical ω and τ(C–H in –CH_2–) = 1299 vs and 1288 m; δ(=C–H, 4-monosubstituted pyridines) = 1234 w and 1081 w; ρ(=C–H) = 1044 w; ring breathing modes (C=C plus C=N) = 1021 s and 1011 m; γ(=C–H, 4-monosubstituted pyridines) = 775 m; depolarized δ(C=C) band for substituted aromatic rings = 659 m and 574 w.

RESULTS AND DISCUSSION

Crystal structure of $[Cd_4(BPY)_5(NTA)_2(H_2O)_4]\cdot(NO_3)_2\cdot(H_2O)_x$ (CUmof-7)

The reaction of $Cd(NO_3)_2$ with BPY and H_3NTA under hydrothermal conditions leads to the formation of colourless crystal plates shown by single-crystal x-ray diffraction to be $[Cd_4(BPY)_5(NTA)_2(H_2O)_4]\cdot(NO_3)_2\cdot(H_2O)_x$ (CUmof-7) (Table 1). This cadmium–organic framework (Cd–OF) contains four crystallographically unique metal centres which appear in both hexa- [Cd(1) and Cd(4)] and heptacoordinated [Cd(2) and Cd(3)] environments, showing distorted regular and capped octahedral coordination geometries, respectively [Fig. 1(b) and Tables 2 and 3]. All the cadmium ions have one solvent molecule and two 4-pyridyl groups (from BPY) in their coordination sphere, with the average Cd—O and Cd—N distances

Table 1. Crystal data and structure refinement details for CUmof-7 and CUmof-8

	CUmof-7	CUmof-8
Formula	$Cd_4C_{62}H_{60}N_{14}O_{22}\cdot xH_2O$	$Cd_4C_{62}H_{88}N_{14}O_{36}$
Formula weight	901.42	2055.06
Crystal system	Triclinic	Monoclinic
Space group	$P\bar{1}$	$P2_1/c$
a (Å)	15.7479(11)	14.6911(2)
b (Å)	16.8667(12)	11.9018(2)
c (Å)	20.6392(10)	23.3036(3)
α (°)	108.382(4)	90
β (°)	96.212(4)	99.952(2)
γ (°)	116.624(2)	90
Volume (Å^3)	4445.0(5)	4013.33(10)
Z	2	2
D_c (g cm^{-3})	1.347	1.701
μ (Mo Kα) (mm^{-1})	1.011	1.143
Crystal size (mm)	$0.18 \times 0.10 \times 0.05$	$0.18 \times 0.16 \times 0.07$
Crystal type	Colourless plates	Colourless plates
θ range	3.55–22.47	3.54–21.03
Index ranges	$-16 \le h \le 16$ $-17 \le k \le 17$ $-21 \le l \le 22$	$-14 \le h \le 14$ $-11 \le k \le 12$ $-23 \le l \le 23$
Reflections collected	26646	19847
Independent reflections	11261 ($R_{int} = 0.0765$)	4295 ($R_{int} = 0.0382$)
Final R indices	$R1 = 0.1376$	$R1 = 0.0583$
$[I > 2\sigma(I)]$	$wR2 = 0.3450$	$wR2 = 0.1650$
Final R indices	$R1 = 0.1610$	$R1 = 0.0633$
(all data)	$wR2 = 0.3668$	$wR2 = 0.1703$
Largest diff. peak and hole	8.559 and -1.256 e Å^{-3}	3.024 and -1.967 e Å^{-3}

being similar at ca 2.35 Å, consistent with reported results for other Cd–OFs.[43–45]

The polydentate NTA^{3-} ligand establishes bridges between three different metal centres in the crystal structure [Cd(1)—Cd(3)—Cd(4) and Cd(4)—Cd(2)—Cd(1)], leading to the formation of $[\cdots Cd(1)\cdots Cd(3)\cdots Cd(4)\cdots Cd(2)\cdots]_n$ chains, distributed along the b direction [see Fig. 1(a) for cadmium-to-cadmium distances]. In the two NTA–Cd moieties [with Cd(2) and Cd(3)] the N-donor atom from the ligand occupies the seventh capping position of the coordination geometry, with an average bite angle of ca 68.9° [Fig. 1(b)]. Each carboxylate group from NTA^{3-} shows a different coordination mode: *anti*-unidentate [for C(66) and C(74)], *syn*, *anti*-bridging [for C(62) and C(76)] and bridging-η^2-*syn*, *syn*-chelate [for C(64) and C(72)]. To our knowledge, this is the first report of a MOF in which NTA^{3-} residues, with such a variety of coordination modes, act as an effective bridge between three crystallographically unique different metal centres.

The Cd(3) and Cd(4) metal centres each have in their coordination sphere one unidentate BPY ligand [N(32)- and N(51)-pyridyl groups] [Fig. 1(b)]. The other N-donor atoms from these unidentate BPYs are probably directly involved in hydrogen bonding with water molecules in the crystal structure. The most important feature of BPY in CUmof-7 is their function as a ditopic ligand: they connect Cd(1) to Cd(2) from different metal chains [$d = 11.679(2)$ Å], forming a plane pseudo-hexagonal (6,3) net; they also establish bridges between two of these sheets, leading to the formation of a bilayer topology [Cd(1)$\cdots$Cd(2)^{i} 11.7234(19) Å and Cd(3)$\cdots$Cd(4)^{ii} 11.7022(19) Å; symmetry codes: (i) $1-x, -y, 2-z$; (ii) $2-x, 1-y, 2-z$] [Fig. 1(a)]. The crystal structure of CUmof-7 is thus best described as an infinite 2D cationic bilayer placed in the *ab* plane and with an empirical formula $[Cd_4(BPY)_5(NTA)_2(H_2O)_4]_n^{2n+}$. This bilayer is perforated by distorted square pores which most probably contain two nitrate ions per formula unit in order to compensate for the positive charge of the framework [Fig. 1(a)]. These two anions were located by the difference Fourier method and refined with geometry heavily restrained.

Bilayers are stacked in an [ABAB...] manner along the c direction (Fig. 2a), and are interconnected through hydrogen bonds between the uncoordinated oxygen atoms from the C(66) and C(74) carboxylate groups (which act as bifurcated acceptors) and the coordinated water molecules in the neighbouring bilayers [Table 4 and Fig. 2 (b)]. Interactions between adjacent bilayers are also further established by face-to-face π–π contacts between the unidentate BPYs coordinated to Cd(3) [average close contact distance ca 3.4 Å; Fig. 3 (a)]. The same type of close contacts can also be found within the bilayers between these same unidentate and the Cd(1)-to-Cd(2) bridging BPYs [Fig. 3(b)].

CUmof-7 contains tubular channels running along the c direction with an average diameter of ca 5.0 Å, considering van der Waals radii for the atoms (Figs 4

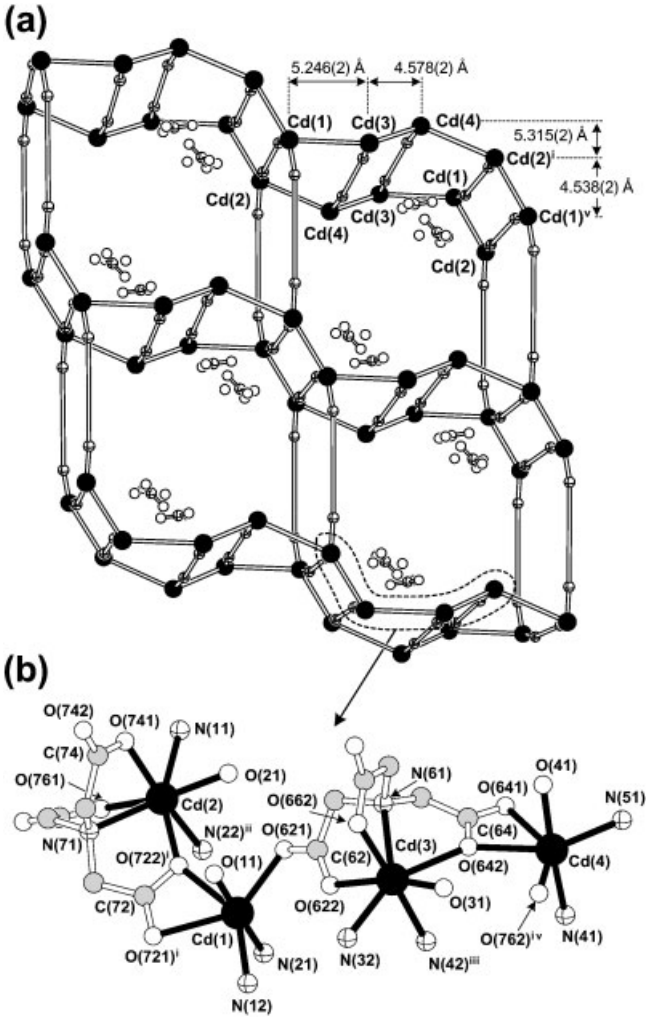

Figure 1. (a) Schematic representation of the cationic $[Cd_4(BPY)_5(NTA)_2(H_2O)_4]_n^{2n+}$ bilayer present in CUmof-7. Nitrate ions and oxygen atoms of the free solvent molecules are also shown. Cd–Cd direct connections mean NTA bridges and N–N represent the BPY ligand. (b) Coordination environments for the four crystallographically unique metal centres. For bond distances (in Å) and angles (in degrees), see Tables 2 and 3, respectively. Symmetry codes: (i) $x+1$, y, z; (ii) $-x+1$, $-y$, $-z+2$; (iii) $-x+2$, $-y+1$, $-z+2$; (iv) $x+1$, $y+1$, z; (v) $x-1$, y, z

and 5). A search for the solvent-accessible voids within the structure using the PLATON[46] software package (1.20 Å probe radius) gives 1244.5 Å^3 (28.0% of the volume of the unit cell). These channels contain a considerable diffuse electron density that proved to be very difficult to resolve. The remaining Q peaks probably correspond to highly disordered solvent molecules from which only one oxygen atom was satisfactorily refined.

Crystal structure of $[Cd_4(BPY)_4(NTA)_2(H_2O)_{10}]\cdot(BPY)\cdot(NO_3)_2\cdot(H_2O)_8$ (CUmof-8)

CUmof-7, directly obtained from the hydrothermal synthesis, is a thermodynamically unstable Cd–OF, and

Table 2. Selected bond lengths for CUmof-7[a]

Bond	Length (Å)	Bond	Length (Å)
Cd(1)—O(621)	2.220(12)	Cd(3)—O(662)	2.336(12)
Cd(1)—N(12)	2.306(9)	Cd(3)—O(31)	2.358(13)
Cd(1)—N(21)	2.321(8)	Cd(3)—N(42)^{iii}	2.380(9)
Cd(1)—O(11)	2.324(15)	Cd(3)—O(622)	2.390(13)
Cd(1)—O(722)^{i}	2.346(12)	Cd(3)—N(32)	2.414(10)
Cd(1)—O(721)^{i}	2.475(14)	Cd(3)—O(642)	2.424(13)
Cd(2)—O(21)	2.350(13)	Cd(3)—N(61)	2.453(15)
Cd(2)—N(11)	2.356(9)	Cd(4)—O(762)^{iv}	2.235(12)
Cd(2)—O(741)	2.380(12)	Cd(4)—N(51)	2.290(10)
Cd(2)—O(761)	2.388(12)	Cd(4)—N(41)	2.302(9)
Cd(2)—N(22)^{ii}	2.391(8)	Cd(4)—O(41)	2.344(14)
Cd(2)—O(722)	2.399(12)	Cd(4)—O(642)	2.344(13)
Cd(2)—N(71)	2.462(14)	Cd(4)—O(641)	2.471(14)

[a] Symmetry codes: (i) $x+1$, y, z; (ii) $-x+1$, $-y$, $-z+2$; (iii) $-x+2$, $-y+1$, $-z+2$; (iv) $x+1$, $y+1$, z.

was converted into another highly crystalline product, also analysed by single-crystal x-ray diffraction and formulated as $[Cd_4(BPY)_4(NTA)_2(H_2O)_{10}]\cdot(BPY)\cdot(NO_3)_2\cdot(H_2O)_8$ (CUmof-8) (Table 1). The CHN composition and x-ray powder diffraction analysis (see Supporting Information, available at the epoc website at http://www.wiley.com/epoc) are in very good agreement with the theoretical calculations based on single-crystal data, confirming phase purity and homogeneity of the bulk. CUmof-8 contains only two crystallographically unique cadmium ions, both present with a seven-coordination geometry, $\{CdO_5N_2\}$ (Fig. 6 and Tables 5 and 6). Cd(1) is coordinated to two water molecules, one BPY and to all possible coordination sites of the polydentate NTA^{3-}, with a coordination geometry best described as a capped octahedron, just as that observed for CUmof-7 in the Cd–NTA moieties (the seventh capping position is here also occupied by the *N*-donor atom from NTA^{3-}). Cd(2) coordination geometry resembles a pentagonal bipyramid, with the equatorial plane being formed by three water molecules and a carboxylate group from NTA^{3-} [C(34)], connected in a slightly asymmetric η^2-*syn*, *syn*-chelate coordination fashion (Table 5). Two *N*-donor atoms from bridging-BPY ligands are *trans*-coordinated in the axial positions.

Just as in the previous structure (and also in CUmof-2 with the HDTPA^{4-} ligand),[29] NTA^{3-} appears in CUmof-8 as a polydentate ligand which completely traps the Cd(1) metal ion inside three five-membered rings (NTA–Cd moiety), formed by the carboxylate groups in an *anti*-unidentate coordinative fashion (Fig. 6). The average bite angle for NTA^{3-} is ca 70.1° (Table 6), whereas for HDTPA^{4-} (in CUmof-2) it is ca 73.0°. C(34) carboxylate group also establishes a bridge to Cd(2) through the formation of a η^2-*syn*, *syn*-chelate with this metal centre [Fig. 6, Cd(1)···Cd(2) 4.8495(9) Å]. Interestingly, all the carboxylate groups maintain the equivalence in the C–O bonds, with the distances in the 1.24–1.26 Å range (Table 5). This is particularly unexpected for the

Table 3. Selected bond angles for CUmof-7[a]

Bond	Angle (°)	Bond	Angle (°)
O(621)—Cd(1)—N(21)	94.2(4)	O(662)—Cd(3)—O(31)	81.2(4)
N(12)—Cd(1)—N(21)	87.5(4)	O(662)—Cd(3)—N(42)^{iii}	175.9(4)
O(621)—Cd(1)—O(11)	85.9(5)	O(31)—Cd(3)—N(42)^{iii}	97.3(4)
N(12)—Cd(1)—O(11)	90.1(5)	O(31)—Cd(3)—O(622)	166.3(5)
N(21)—Cd(1)—O(11)	176.9(5)	N(42)^{iii}—Cd(3)—O(622)	81.7(4)
O(621)—Cd(1)—O(722)^{i}	84.1(4)	O(662)—Cd(3)—N(32)	86.7(5)
N(21)—Cd(1)—O(722)^{i}	98.5(4)	O(31)—Cd(3)—N(32)	81.4(4)
O(11)—Cd(1)—O(722)^{i}	84.6(5)	N(42)^{iii}—Cd(3)—N(32)	89.3(5)
N(12)—Cd(1)—O(721)^{i}	87.8(4)	O(622)—Cd(3)—N(32)	84.9(5)
N(21)—Cd(1)—O(721)^{i}	92.9(4)	O(31)—Cd(3)—O(642)	75.3(4)
O(11)—Cd(1)—O(721)^{i}	89.0(5)	N(42)^{iii}—Cd(3)—O(642)	76.5(4)
O(21)—Cd(2)—N(11)	83.1(4)	N(32)—Cd(3)—O(642)	150.7(4)
O(21)—Cd(2)—O(741)	79.5(4)	O(31)—Cd(3)—N(61)	121.6(5)
N(11)—Cd(2)—O(741)	82.3(4)	N(42)^{iii}—Cd(3)—N(61)	114.5(5)
O(21)—Cd(2)—O(761)	165.8(4)	N(32)—Cd(3)—N(61)	141.7(5)
N(11)—Cd(2)—O(761)	82.8(4)	O(762)^{iv}—Cd(4)—N(51)	129.7(4)
O(21)—Cd(2)—N(22)^{ii}	99.1(4)	O(762)^{iv}—Cd(4)—N(41)	94.3(4)
N(11)—Cd(2)—N(22)^{ii}	92.8(4)	N(51)—Cd(4)—N(41)	87.0(5)
O(741)—Cd(2)—N(22)^{ii}	175.0(4)	O(762)^{iv}—Cd(4)—O(41)	84.5(5)
O(761)—Cd(2)—N(22)^{ii}	79.8(4)	N(51)—Cd(4)—O(41)	90.5(5)
O(21)—Cd(2)—O(722)	77.2(4)	N(41)—Cd(4)—O(41)	175.6(5)
N(11)—Cd(2)—O(722)	156.9(4)	O(762)^{iv}—Cd(4)—O(642)	83.9(5)
N(22)^{ii}—Cd(2)—O(722)	78.6(4)	N(51)—Cd(4)—O(642)	145.4(4)
O(21)—Cd(2)—N(71)	122.6(5)	N(41)—Cd(4)—O(642)	99.9(5)
N(11)—Cd(2)—N(71)	134.6(4)	O(41)—Cd(4)—O(642)	84.2(5)
N(22)^{ii}—Cd(2)—N(71)	115.6(4)	O(762)^{iv}—Cd(4)—O(641)	138.6(5)
		N(51)—Cd(4)—O(641)	91.1(5)
		N(41)—Cd(4)—O(641)	94.6(4)
		O(41)—Cd(4)—O(641)	89.0(5)

[a] Symmetry codes: (i) $x+1$, y, z; (ii) $-x+1$, $-y$, $-z+2$; (iii) $-x+2$, $-y+1$, $-z+2$; (iv) $x+1$, $y+1$, z.

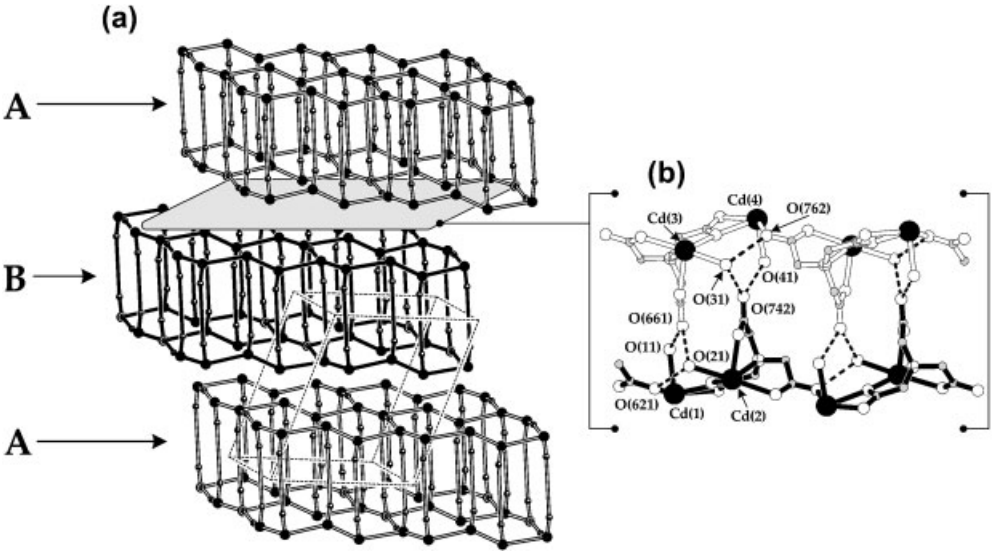

Figure 2. (a) Parallel stacking of the cationic $[Cd_4(BPY)_5(NTA)_2(H_2O)_4]_n^{2n+}$ bilayers in an [ABAB...] fashion along the c direction. (b) Magnified view of the inter-bilayer space, showing the hydrogen-bonding network (dashed lines) between two adjacent bilayers (white- and black-filled bonds). H-atoms have been omitted for simplicity. For hydrogen-bonding geometry, see Table 4

anti-unidentate carboxylate groups [C(32) and C(62)] and can be explained by the presence of strong hydrogen bonds (Table 7).[47]

Similarly to CUmof-2, this Cd–OF can also be seen as the self-assembly of a bimetallic secondary building unit (SBU) into a cationic chain, $[Cd_2(BPY)_2(NTA)(H_2O)_5]_n^{n+}$, which runs along the c direction (Fig. 7). Once again, BPY appears with a variety of coordination fashions. Ditopic bridging BPY also acts as the physical links between SBUs, connecting consecutive Cd(2) metal

Table 4. Hydrogen-bonding geometry for CUmof-7[a]

D···A	d(D···A) (Å)	∠(D—H···A) (°)
O(11)···O(661)^{i}	2.740(20)	163(2)
O(21)···O(661)^{ii}	2.707(19)	167(1)
O(21)···O(621)^{iii}	2.788(17)	128(1)
O(31)···O(742)^{iv}	2.732(19)	149(1)
O(31)···(O762)^{v}	2.737(18)	155(2)
O(41)···(O742)^{vi}	2.716(19)	167(2)
O(1W)···(O104)^{vi}	2.58(6)	—

[a]Symmetry codes: (i) $-x+2, -y, -z+1$; (ii) $-x+1, -y, -z+1$; (iii) $x-1$, y, z; (iv) $x+1, y+1, z$; (v) $-x+2, -y+1, -z+1$; (vi) $x, y, z-1$.

centres [Cd(2)···Cd(2)^{i} 11.6769(2) Å, symmetry code: (i) x, $1/2-y$, $1/2+z$]. The NTA–Cd moiety is also coordinated to a unidentate BPY, which is hydrogen bonded to a coordinated water molecule (O23) from an adjacent SBU (Table 7). However, in this crystal structure, the 4-pyridyl groups for both coordinated BPYs are not coplanar as in CUmof-2, with dihedral angles of 31.3(14) and 27.6(14)° for the ditopic bridging and unidentate fashions, respectively (Figs 7 and 9). A third type of BPY can also be found in CUmof-8, lying in a centre of symmetry and not being coordinated to a metal centre. Instead, it is involved in hydrogen bonds with the O(21) water molecules (Figs 8 and 9, Table 7). Bridges between adjacent $[Cd_2(BPY)_2(NTA)(H_2O)_5]_n^{n+}$ cationic chains are assured only by the hydrogen-bonding network present in the crystal structure (Figs 8 and 9). Once again, the polydentate NTA^{3-} seems to prevent coordinative connections between adjacent chains, directing the growth of the Cd–OF through the core of the SBU.[29]

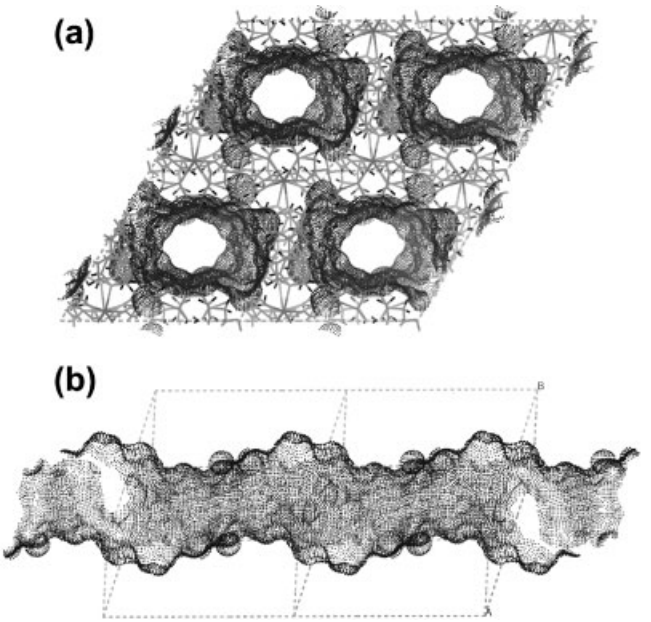

Figure 4. (a) Projection of the crystal structure of CUmof-7 in the *ab* plane revealing the presence of large tunnels. (b) Perspective view enhancing the shape of the tunnels. Images created by generating Connolly surfaces (1.4 Å probe radius and 8.0 dot density) using the software package Cerius[2,55]

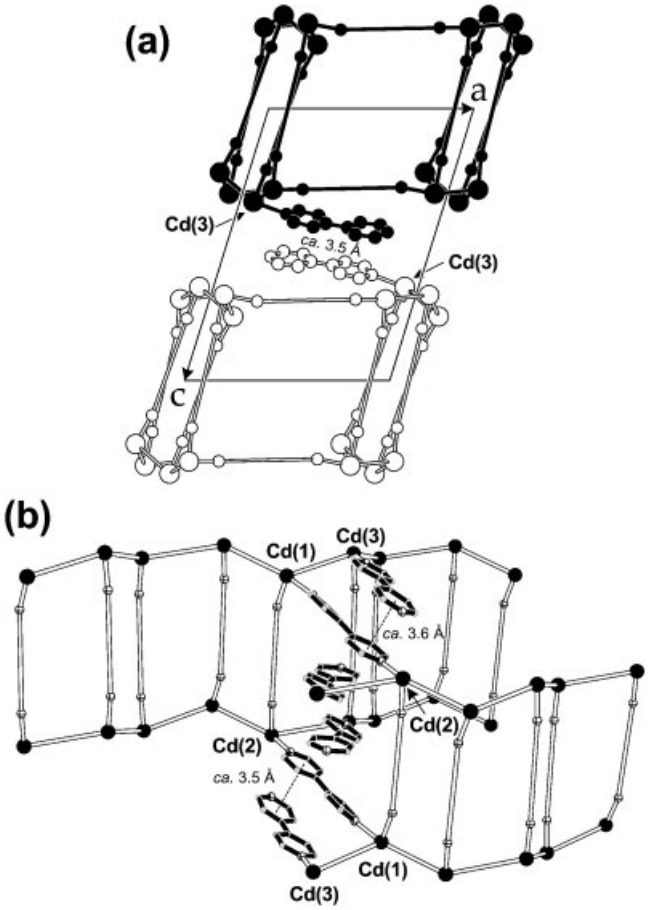

Figure 3. Close π–π contacts between the BPY ligands: (a) between adjacent bilayers; (b) within the bilayers and between the unidentate and the Cd(1)-to-Cd(2)- bridging BPYs

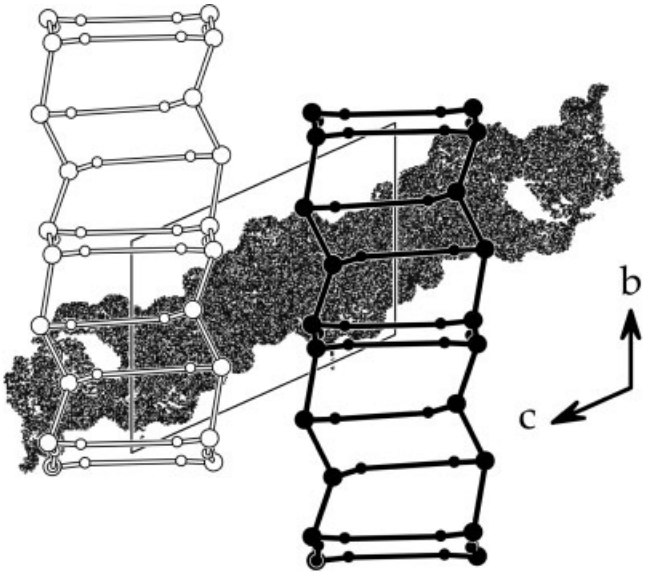

Figure 5. View along the *a* axis showing the parallel packing of two bilayers and the tunnels which run along the *c* direction

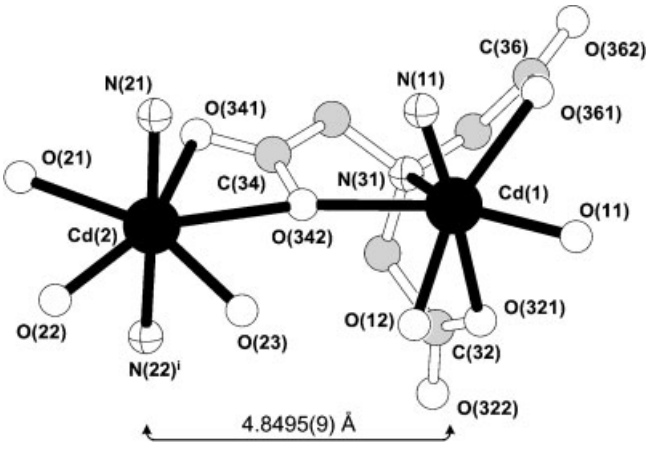

Figure 6. Coordination environments for the two crystallographically unique metal centres in CUmof-8. For symmetry codes and bond distances (in Å) and angles (in degrees), see Tables 5 and 6, respectively

Table 5. Selected bond lengths for CUmof-8[a]

Bond	Length (Å)	Bond	Length (Å)
Cd(1)—O(11)	2.288(7)	Cd(2)—N(21)	2.314(7)
Cd(1)—O(321)	2.322(7)	Cd(2)—N(22)^{i}	2.319(7)
Cd(1)—N(11)	2.343(8)	Cd(2)—O(22)	2.344(6)
Cd(1)—O(342)	2.403(6)	Cd(2)—O(21)	2.361(6)
Cd(1)—N(31)	2.403(8)	Cd(2)—O(23)	2.392(6)
Cd(1)—O(361)	2.415(7)	Cd(2)—O(341)	2.409(7)
Cd(1)—O(12)	2.563(7)	Cd(2)—O(342)	2.565(6)
C(32)—O(321)	1.259(14)	C(34)—O(342)	1.265(11)
C(32)—O(322)	1.259(14)	C(36)—O(362)	1.247(12)
C(34)—O(341)	1.244(11)	C(36)—O(361)	1.263(12)

[a] Symmetry codes: (i) x, ½−y, ½+z.

FT-IR and FT-Raman spectroscopy confirm the presence of the two organic ligands used in the synthesis (through the typical vibrations of substituted pyridines and aliphatic —CH_2— groups), and also the nitrate ion (typical stretching vibrations at 1436 cm^{-1}). The extensive hydrogen-bonding network present in CUmof-8 is also evident in the spectra, not only through the presence of the typical O–H stretching vibrations for water molecules (very broad band), but also to the in-plane ($\delta = 1357\ cm^{-1}$) and out-of-plane ($\gamma = 926$ and 905 cm^{-1}) O–H···O deformations.[48] FT-IR also reveals the characteristic antisymmetric (1602 and 1574 cm^{-1}) and symmetrical (1412 and 1385 cm^{-1}) stretching bands of carboxylate ions. The corresponding $\Delta[\nu_{asym}(CO_2) - \nu_{sym}(CO_2)]$ values are 217 and 162 cm^{-1}, which is a clear indication of the presence of carboxylate groups in the *anti*-unidentate and bridging-η^2-*syn*, *syn*-chelate coordination modes, respectively, as is described by the crystal structure.[47,49]

Thermal analysis shows that the thermal stability of CUmof-8 is much smaller than usually found for MOFs. The first weight loss (15.7%) occurs in the 20–115 °C temperature range, and corresponds to the release of all the water molecules (15.8%, calculated). Despite the strong and very extensive hydrogen-bonding network present in CUmof-8, the kinetics of this dehydration process are relatively fast, in contrast to what happens in CUmof-1.[28] Between 115 °C and 500 °C there are several weight losses and, owing to the extreme complexity of the crystal structure, it is not feasible to characterize each decomposition fully. However, the sample seems to undergo complete oxidation to form cadmium(II) oxide as the final residue: the final 24.9% of residue obtained in

Table 6. Selected bond angles for CUmof-8[a]

Bond	Angle (°)	Bond	Angle (°)
O(11)—Cd(1)—O(321)	87.9(3)	N(21)—Cd(2)—N(22)^{i}	178.7(3)
O(11)—Cd(1)—N(11)	88.4(3)	N(21)—Cd(2)—O(22)	91.5(3)
O(321)—Cd(1)—N(11)	168.4(3)	N(22)^{i}—Cd(2)—O(22)	87.4(3)
O(11)—Cd(1)—O(342)	151.0(2)	N(21)—Cd(2)—O(21)	89.6(2)
O(321)—Cd(1)—O(342)	98.7(2)	N(22)^{i}—Cd(2)—O(21)	89.4(3)
N(11)—Cd(1)—O(342)	79.5(2)	O(22)—Cd(2)—O(21)	77.7(2)
O(11)—Cd(1)—N(31)	139.5(3)	N(21)—Cd(2)—O(23)	92.4(2)
O(321)—Cd(1)—N(31)	71.1(3)	N(22)^{i}—Cd(2)—O(23)	88.2(2)
N(11)—Cd(1)—N(31)	118.1(3)	O(22)—Cd(2)—O(23)	77.3(2)
O(342)—Cd(1)—N(31)	68.5(2)	O(21)—Cd(2)—O(23)	154.9(2)
O(11)—Cd(1)—O(361)	83.2(2)	N(21)—Cd(2)—O(341)	91.3(2)
O(321)—Cd(1)—O(361)	105.7(3)	N(22)^{i}—Cd(2)—O(341)	89.3(2)
N(11)—Cd(1)—O(361)	84.8(3)	O(22)—Cd(2)—O(341)	156.3(2)
O(342)—Cd(1)—O(361)	121.3(2)	O(21)—Cd(2)—O(341)	78.8(2)
N(31)—Cd(1)—O(361)	70.6(2)	O(23)—Cd(2)—O(341)	126.1(2)
O(11)—Cd(1)—O(12)	74.9(2)	N(21)—Cd(2)—O(342)	96.3(2)
O(321)—Cd(1)—O(12)	80.5(3)	N(22)^{i}—Cd(2)—O(342)	85.0(2)
N(11)—Cd(1)—O(12)	87.8(3)	O(22)—Cd(2)—O(342)	150.3(2)
O(342)—Cd(1)—O(12)	78.4(2)	O(21)—Cd(2)—O(342)	130.8(2)
N(31)—Cd(1)—O(12)	131.5(3)	O(23)—Cd(2)—O(342)	73.8(2)
O(361)—Cd(1)—O(12)	157.1(2)	O(341)—Cd(2)—O(342)	52.4(2)

[a] Symmetry codes: (i) x, ½−y, ½+z.

Table 7. Hydrogen-bonding geometry for CUmof-8[a]

D···A	d(D···A) (Å)	∠(D—H···A) (°)
O(11)···O(321)	3.200(10)	124(6)
O(11)···O(362)^{i}	2.836(10)	—
O(12)···O(4W)	2.715(13)	106(7)
O(12)···O(361)^{i}	2.923(10)	115(6)
O(21)···O(1W)	2.941(13)	160(9)
O(21)···N(41)	2.807(11)	165(9)
O(22)···O(362)^{ii}	2.731(10)	173(8)
O(22)···O(1W)^{iii}	2.787(13)	161(9)
O(23)···N(12)^{iv}	2.728(10)	161(7)
O(23)···O(342)	2.978(9)	119(7)
O(1W)···O(2W)	2.855(16)	—
O(1W)···O(341)	2.733(13)	—
O(2W)···O(103)^{iii}	3.01(2)	—
O(2W)···O(3W)	2.941(16)	—
O(3W)···O(101)	2.87(2)	—
O(3W)···O(322)^{v}	2.949(16)	—
O(4W)···O(322)^{vi}	2.721(15)	—
O(4W)···O(321)	2.848(14)	—

[a] Symmetry codes: (i) $-x+1, -y, -z$; (ii) $x, 1+y, z$; (iii) $-x, -y, -z$; (iv) $x, ½-y, ½+z$; (v) $-x, ½+y, ½-z$; (vi) $1-x, ½-y, 1-z$.

the analysis is in good agreement with the expected value considering the formation of the stoichiometric amount of CdO (25.0%).

CONCLUSIONS

Two cadmium–organic frameworks containing the polydentate nitrilotriacetate (NTA^{3-}) organic ligand have been synthesized and characterized structurally. The metastable product directly obtained from the hydrothermal synthesis, CUmof-7, has a 2D framework with a bilayer topology and proved to be very unstable, undergoing a structural transformation into CUmof-8 over a period of a few weeks. The crystal structure of this compound contains a 1D cationic polymer, and confirms the general assumption (based on a search in the Cambridge CSD) that NTA^{3-} preferentially leads to the synthesis of low-dimensional MOFs. As expected, CUmof-8 shows striking similarities to CUmof-2, confirming the ability of NTA^{3-} to remove coordination sites and direct the growth of the MOF.

EXPERIMENTAL

Structure determination using single-crystal x-ray diffraction. X-ray diffraction data were collected from suitable single crystals directly obtained from the mother liquors and mounted on a glass fibre using perfluoropolyether oil.[50] Diffraction intensities were collected at 180(2) K on a Nonius KappaCCD diffractrometer with Mo Kα monochromated radiation ($\lambda = 0.7107$ Å). The structure was solved with the direct methods of SHELXS-97[51] and refined by full-matrix least squares on F^2 using SHELXL-97 with anisotropic displacement parameters for all non-hydrogen atoms.[52] Multi-scan absorption corrections were also applied.[53] Hydrogen atoms bound to carbon were generated geometrically and refined using a riding model with an isotropic displacement parameter fixed at 1.2 times U_{eq} for the atom to which they are attached. All cavity dimensions were calculated by overlapping rigid spheres with van der Waals radii for each element: Cd^{2+}, 2.20 Å; O, 1.52 Å; N, 1.55 Å; C, 1.70 Å. Hydrogen atoms were omitted in all cases for simplicity. Crystallographic data collection and structure refinement are summarized in Table 1, and selected bond lengths, angles and a full description of the hydrogen-bonding geometry are present in Tables 2–7. Fractional atomic coordinates (including H-atoms) and displacement

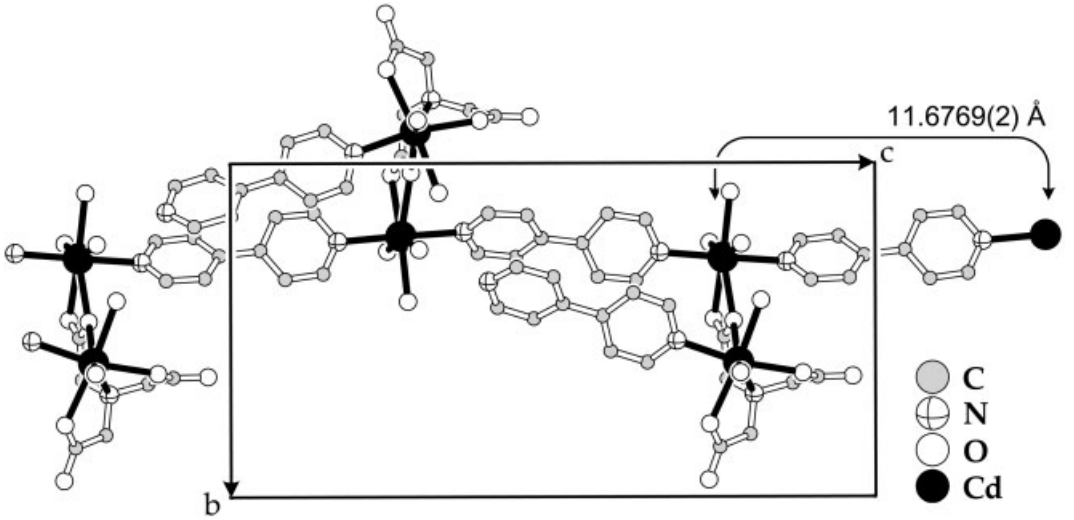

Figure 7. View of the $[Cd_2(BPY)_2(NTA)(H_2O)_5]_n^{n-}$ cationic chain present in CUmof-8, constructed from the repetition of the bimetallic SBU along the c direction. H-atoms have been omitted for clarity

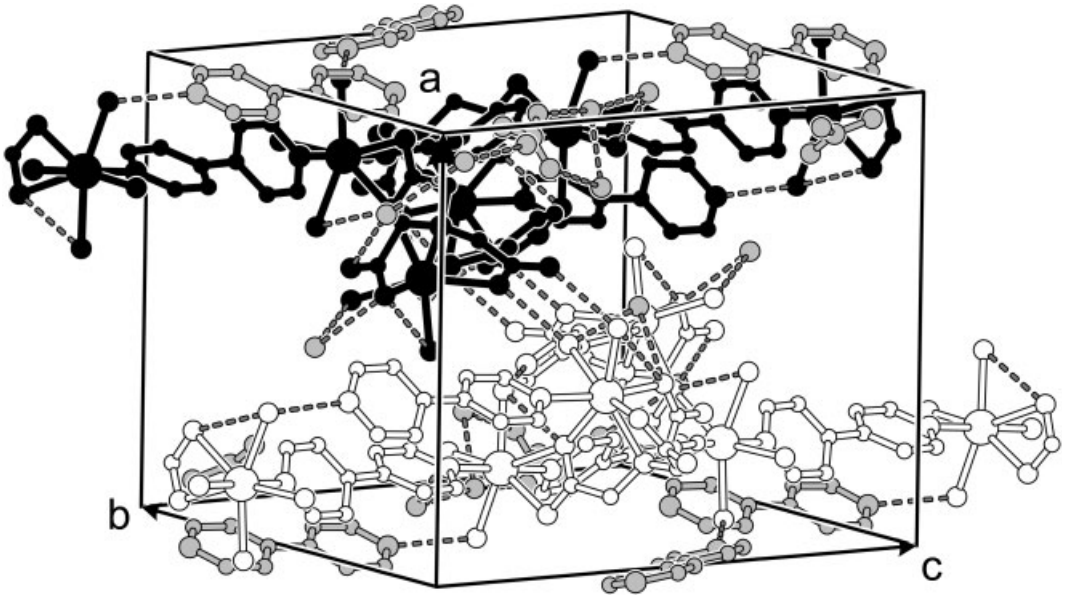

Figure 8. Perspective view of CUmof-8, showing the hydrogen-bonding network (dashed lines) between two adjacent $[Cd_2(BPY)_2(NTA)(H_2O)_5]_n^{n-}$ cationic chains (white and black bonds). Uncoordinated BPY, water molecules and nitrate ions are drawn with grey-filled bonds. H-atoms have been omitted for simplicity. For hydrogen-bonding geometry, see Table 7

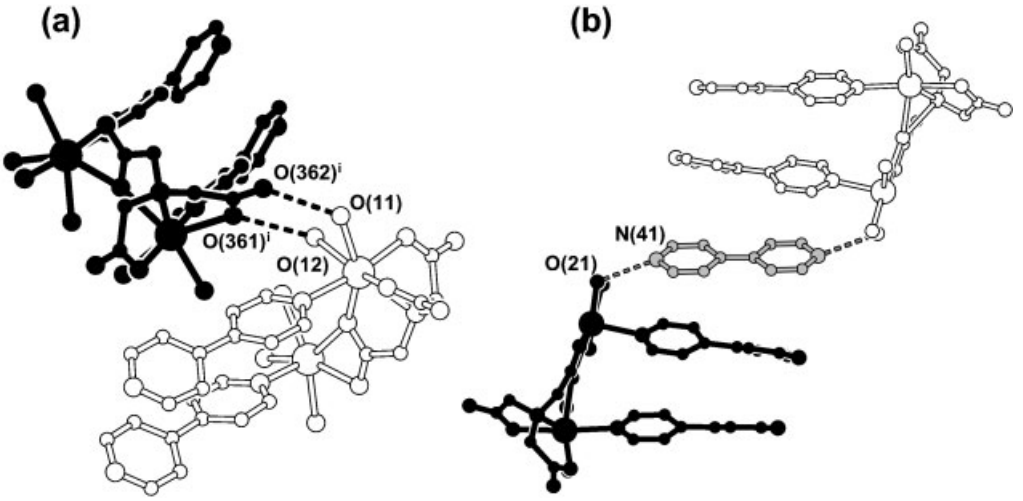

Figure 9. View in detail of the hydrogen bonds (dashed lines) between SBUs from adjacent $[Cd_2(BPY)_2(NTA)(H_2O)_5]_n^{n-}$ cationic chains (white and black-filled bonds). Uncoordinated BPY molecules are drawn with grey-filled bonds. For hydrogen-bonding geometry and symmetry codes, see Table 7

parameters are supplied as Electronic Supplementary Information (ESI) to this paper (available at the epoc website at http://www.wiley.com/epoc). Crystallographic data (excluding structure factors) for the structures reported in this paper have been deposited with the Cambridge Crystallographic Data Centre as supplementary publication No. CCDC-202444 and 202445.

Refinement details for CUmof-7. Framework atoms were located and refined with isotropic displacement parameters, except for Cd^{2+} centres, which were refined anisotropically. This refinement strategy was based upon the fact that anisotropic treatment for almost all non-H atoms of the framework does not lead to significant improvements in either the residual electron density (largest diff. peak $= 8.348$ e Å^{-3}) or the R factors {e.g. $R1[I > 2\sigma(I)] = 0.1314$ and $wR2$(all data) $= 0.3532$}. Also, and in particular for the uncoordinated 4-pyridyl groups, some carbon atoms are then refined as prolates or oblates.

AFIX 66 was applied to all 4-pyridyl rings. Hydrogen atoms bound to coordinated water molecules were refined using O—H distances restrained to 0.84(1) Å, H···H distances restrained to 1.37(2) Å and U_{iso} constrained to 1.2 times U_{eq} for the oxygen to which they are attached. The considerable diffuse electron density inside the

channels was very difficult to resolve, with the 2-charge required per formula unit to balance the framework being most probably present as two nitrate anions. The two NO_3^- anions were located with the difference Fourier method and refined with geometry heavily restrained. All other Q peaks are probably disordered solvent molecules. Two oxygen atoms were refined satisfactorily but no attempt was made to place the hydrogen atoms on these.

Refinement details for CUmof-8. Bond distance restraints were not applied except for the hydrogen atoms associated with the coordinated solvent molecules, for which the O—H and H···H distances have been restrained to be 0.88(1) and 1.44(1) Å, respectively. These restraints ensure a chemically reasonable geometry for the coordinated water molecule. Four additional uncoordinated water molecules were refined satisfactorily with a single isotropic displacement parameter common to all O-atoms (no attempt was made to place the H-atoms on these water molecules). One NO_3^- anion was located from difference Fourier maps and refined with another single isotropic displacement parameter common to all four atoms (O and N).

Other techniques. X-ray powder diffraction patterns were measured at ambient temperature on a STOE STADI-P high-resolution transmission diffractometer with Ge(111)-monochromated Cu Kα radiation ($\lambda =$ 1.5406 Å), and a position-sensitive detector covering a 6° 2θ angle (40 kV, 40 mA). Data were collected using the step counting method (step 0.5 °, time 460 s) in the range $2 \leq 2\theta^\circ \leq 60$. Simulated powder patterns were based on single-crystal data and performed with the STOE Win XPOW software package.[54]

Thermogravimetric analysis (TGA) was carried out using a Shimadzu TGA-50 instrument with a heating rate of 10 °C min^{-1}, under a nitrogen atmosphere with a flow-rate of 20 cm^3 min^{-1}. FT-IR spectra were collected using KBr pellets (Aldrich, 99% +, FT-IR grade) on a Mattson 7000 FT-IR spectrometer. FT-Raman spectra were measured on a Bruker RFS 100 instrument with an Nd:YAG coherent laser ($\lambda = 1064$ nm).

Elemental analysis for carbon (C), nitrogen (N) and hydrogen (H) was performed on an Exeter Analytical CE-440 Elemental Analyser, where the sample was combusted under an oxygen atmosphere at 975 °C for 1 min. Helium was used as purge gas.

Acknowledgements

The authors thank Dr Andrew D. Bond for the crystal solution and the Fundação Para a Ciência e Tecnologia (FCT), Portugal, for financial support for F.A.A.P. through an SFRH/BD/3024/2000 scholarship.

REFERENCES

1. Batten SR, Robson R. *Angew. Chem., Int. Ed. Engl.* 1998; **37**: 1461–1494.
2. Kitagawa S, Kondo M. *Bull. Chem. Soc. Jpn.* 1998; **71**: 1739–1753.
3. Zaworotko MJ. *Chem. Commun.* 2001; 1–9.
4. Chen BL, Eddaoudi M, Reineke TM, Kampf JW, O'Keeffe M, Yaghi OM. *J. Am. Chem. Soc.* 2000; **122**: 11559–11560.
5. Hagrman PJ, Hagrman D, Zubieta J. *Angew. Chem., Int. Ed. Engl.* 1999; **38**: 2639–2684.
6. Yaghi OM, Li HL, Davis C, Richardson D, Groy TL. *Acc. Chem. Res.* 1998; **31**: 474–484.
7. Kitaura R, Fujimoto K, Noro S, Kondo M, Kitagawa S. *Angew. Chem., Int. Ed. Engl.* 2002; **41**: 133–135.
8. Dong YB, Smith MD, Layland RC, zur Loye HC. *Chem. Mater.* 2000; **12**: 1156–1161.
9. Yaghi OM, Li GM, Li HL. *Nature (London)* 1995; **378**: 703–706.
10. Seo JS, Whang D, Lee H, Jun SI, Oh J, Jeon YJ, Kim K. *Nature (London)* 2000; **404**: 982–986.
11. Chui SSY, Lo SMF, Charmant JPH, Orpen AG, Williams ID. *Science* 1999; **283**: 1148–1150.
12. Tong ML, Shi JX, Chen XM. *New J. Chem.* 2002; **26**: 814–816.
13. Zhu HF, Zhao W, Okamura T, Fei BL, Sun WY, Ueyama N. *New J. Chem.* 2002; **26**: 1277–1279.
14. Fei BL, Sun WY, Okamura T, Tang WX, Ueyama N. *New J. Chem.* 2001; **25**: 210–212.
15. Fu ZY, Wu XT, Dai JC, Wu LM, Cui CP, Hu SM. *Chem. Commun.* 2001; 1856–1857.
16. Papaefstathiou GS, Vicente R, Raptopoulou CP, Terzis A, Escuer A, Perlepes SP. *Eur. J. Inorg. Chem.* 2002; 2488–2493.
17. Shova S, Novitchi G, Gdaniec M, Caneschi A, Gatteschi D, Korobchenko L, Voronkova VK, Simonov YA, Turta C. *Eur. J. Inorg. Chem.* 2002; 3313–3318.
18. Muthuraman M, Masse R, Nicoud JF, Desiraju GR. *Chem. Mat.* 2001; **13**: 1473–1479.
19. Yang G, Zhu HG, Liang BH, Chen XM. *J. Chem. Soc., Dalton Trans.* 2001; 580–585.
20. Ezuhara T, Endo K, Matsuda K, Aoyama Y. *New J. Chem.* 2000; **24**: 609–613.
21. Li YG, Zhang H, Wang E, Hao N, Hu CW, Yan Y, Hall D. *New J. Chem.* 2002; **26**: 1619–1623.
22. Pschirer NG, Ciurtin DM, Smith MD, Bunz UHF, zur Loye HC. *Angew. Chem., Int. Ed. Engl.* 2002; **41**: 583–585.
23. Kepert CJ, Prior TJ, Rosseinsky MJ. *J. Am. Chem. Soc.* 2000; **122**: 5158–5168.
24. Teichert O, Sheldrick WS. *Z. Anorg. Allg. Chem.* 2000; **626**: 1509–1513.
25. Fujita M, Kwon YJ, Washizu S, Ogura K. *J. Am. Chem. Soc.* 1994; **116**: 1151–1152.
26. MacDonald JC, Dorrestein PC, Pilley MM, Foote MM, Lundburg JL, Henning RW, Schultz AJ, Manson JL. *J. Am. Chem. Soc.* 2000; **122**: 11692–11702.
27. Gopalakrishnan J. *Chem. Mater.* 1995; **7**: 1265–1275.
28. Paz FAA, Khimyak YZ, Bond AD, Rocha J, Klinowski J. *Eur. J. Inorg. Chem.* 2002; 2823–2828.
29. Paz FAA, Bond AD, Khimyak YZ, Klinowski J. *Acta Crystallogr., Sect. C* 2002; **58**: M608–M610.
30. Paz FAA, Bond AD, Khimyak YZ, Klinowski J. *Acta Crystallogr., Sect. E* 2002; **58**: M691–M693.
31. Paz FAA, Khimyak YZ, Klinowski J. *Acta Crystallogr., Sect. E* 2003; **59**: M8–M10.
32. CSD, Version 5.23, September 2002 (4 updates).
33. Ng SW. *Acta Crystallogr., Sect. C* 1999; **55**: 1447–1449.
34. Malyarick MA, Ilyuhin AB, Petrosyants SP. *Main Group Met. Chem.* 1994; **17**: 707.
35. Fomenko VV, Kopaneva LI, Porai-Koshits MA. *Zh. Strukt. Khim.* 1974; **15**: 268.
36. Battaglia LP, Corradi AB, Tani MEV. *Acta Crystallogr., Sect. B* 1975; **31**: 1160.
37. Fomenko VV, Kopaneva LI, Porai-Koshits MA. *Zh. Strukt. Khim.* 1974; **16**: 645.
38. Ilyukhin AB, Poznyak AL, Sergienko VS, Stopolyanskaya LV. *Kristallografiya* 1998; **43**: 812.

39. Li L, Liu HB, Xu Y, Yin G, Chen JT, Xu Z. *Chem. Lett.* 2001; 214–215.
40. Ilyukhin AB, Davidovich RL, Logvinova VB. *Zh. Neorg. Khim.* 1999; **44**: 193.
41. Oliver JD, Barnett BL, Strickland LC. *Acta Crystallogr., Sect. B* 1984; **40**: 377–381.
42. Whitlow SH. *Inorg. Chem.* 1973; **12**: 2286.
43. Bakalbassis EG, Korabik M, Michailides A, Mrozinski J, Raptopoulou C, Skoulika S, Terzis A, Tsaousis D. *J. Chem. Soc., Dalton Trans.* 2001; 850–857.
44. Evans OR, Lin WB. *Inorg. Chem.* 2000; **39**: 2189–2198.
45. Wang ZY, Xiong RG, Foxman BM, Wilson SR, Lin WB. *Inorg. Chem.* 1999; **38**: 1523–1528.
46. Spek AL. *Acta Crystallogr., Sect. A* 1990; **46**: C34.
47. Oldham C. In *Comprehensive Coordination Chemistry* (1st edn), vol. **2**, Wilkinson SG (ed). Pergamon Press: Oxford, 1987; 435–459.
48. Roeges NPG. *A Guide to the Complete Interpretation of Infrared Spectra of Organic Structures* (4th edn). Wiley: Chichester, 1998.
49. Deacon GB, Phillips RJ. *Coord. Chem. Rev.* 1980; **33**: 227–250.
50. Kottke T, Stalke D. *J. Appl. Crystallogr.* 1993; **26**: 615–619.
51. Sheldrick GM. *SHELXL 97, Program for Crystal Structure Refinement*. University of Göttingen: Göttingen, 1997.
52. Sheldrick GM. *SHELXS 97, Program for Crystal Structure Solution*. University of Göttingen: Göttingen, 1997.
53. Blessing RH. *Acta Crystallogr., Sect. A* 1995; **51**: 33–38.
54. STOE, Hilpert str. 10, D 64295 Darmstadt, Germany *WinXPOW THEO. Version* 1.15. STOE, 1999.
55. *Cerius*^{2}*, Version* 3. Molecular Simulations, San Diego, CA, USA, 1996.

